The Journal of Immunology

Perforin-Dependent Brain-Infiltrating Cytotoxic CD8 $^{+}$ T Lymphocytes Mediate Experimental Cerebral Malaria Pathogenesis

Josianne Nitcheu, Olivia Bonduelle, Christophe Combadiere, Maurel Tefit, Danielle Seilhean, Dominique Mazier and Behazine Combadiere

J Immunol 2003; 170:2221-2228; ;
doi: 10.4049/jimmunol.170.4.2221
http://www.jimmunol.org/content/170/4/2221

The Journal of Immunology is published twice each month by
The American Association of Immunologists, Inc.,
1451 Rockville Pike, Suite 650, Rockville, MD 20852

Print ISSN: 0022-1767 Online ISSN: 1550-6606.

Perforin-Dependent Brain-Infiltrating Cytotoxic CD8$^+$ T Lymphocytes Mediate Experimental Cerebral Malaria Pathogenesis[1]

Josianne Nitcheu,* Olivia Bonduelle,† Christophe Combadiere,† Maurel Tefit,* Danielle Seilhean,‡ Dominique Mazier,[2,3]* and Behazine Combadiere[2,3†]

Experimental cerebral malaria (ECM) resulting from *Plasmodium berghei* ANKA infection involves T lymphocytes. However, the mechanisms of T cell-mediated pathogenesis remain unknown. We found that, in contrast to ECM-susceptible C57BL6 mice, perforin-deficient (PFP-KO) mice were resistant to ECM in the absence of brain lesions, whereas cytoadherence of parasitized erythrocytes and massive accumulation of activated/effector CD8 lymphocytes were observed in both groups of mice. ECM is induced in PFP-KO mice after adoptive transfer of cytotoxic CD8$^+$ cells from infected C57BL6 mice, which were directed to the brain of PFP-KO mice. This specific recruitment might involve chemokine/chemokine receptors, since their expression was up-regulated on activated CD8 cells, and susceptibility to ECM was delayed in CCR5-KO mice. Thus, lymphocyte cytotoxicity and cell trafficking are key players in ECM pathogenesis. ***The Journal of Immunology*, 2003, 170: 2221–2228.**

Cerebral malaria (CM)[4] is one of the most severe complications of *Plasmodium falciparum* infection and the main cause of death in humans (1). The murine model of *Plasmodium berghei* ANKA (*PbA*) reproduces relevant clinical and pathological features of the human disease (2). Although many aspects of the pathogenesis of CM in experimental models have been described, the precise mechanisms leading to this complication are not fully understood. The initial observation of athymic nude mice not developing this neurological syndrome upon infection with *PbA* demonstrated the requirement for T lymphocytes in experimental cerebral malaria (ECM) pathogenesis (3). The respective roles of T cell subsets in the pathogenesis of ECM have been analyzed by depletion of CD4 or CD8 T cells in C57BL/6 mice that did not develop ECM (4). CD8 T lymphocytes are highly involved in ECM pathogenesis, since mice homozygous for the null allele of the β_2-microglobulin gene that lack functional CD8 T cells (4) as well as CD8 knockout (KO) mice (5) were resistant to ECM. In addition, a selective increase in Vβ8$^+$ CD8 T cells has been observed during ECM, suggesting a critical role for the T cell-mediated immune response after *PbA* infection and its neurological consequence (5). However, little is known about the precise mechanisms of CD8 T cell induction of ECM pathogenesis. We investigated the role of cytolytic effector mechanisms mediated by CD8 cells in the development of ECM and the involvement of T lymphocytes in brain cell trafficking. Indeed, in the past years, trafficking of immunocompetent cells has been highly implicated in the establishment of the immune response and disease progression (6). Based on chemokine receptor-deficient mice models, chemokine/chemokine receptors have been recently implicated in various pathologies, such as multiple sclerosis in human or murine experimental autoimmune encephalomyelitis or after transient focal cerebral ischemia (7–10). Indeed, migration of leukocytes to the CNS has been described as a critical factor during experimental autoimmune encephalomyelitis (11–13). In our study we used a variety of bioengineered deficiencies ideal 1) for probing the role of immune elements in cerebral malaria pathogenesis, 2) to investigate the mechanisms by which T cells mediate cerebral malaria pathology, and 3) to analyze the importance of lymphocyte trafficking to the CNS during ECM pathogenesis.

Materials and Methods

Mice

Six- to 8-wk-old female C57BL/6 wild-type (WT) mice were purchased from Charles River Breeding Laboratories (Saint-Aubin les Elbeufs, France). Age-matched perforin-deficient mice (PFP-KO), *lpr* (Fas-natural mutation-inducing lymphoproliferative disease), and *gld* (Fas-ligand natural mutation-inducing generalized lymphadenopathy) mice on the C57BL6 background were obtained from The Jackson Laboratory (Bar Harbor, ME) and bred in our animal facilities (Nouvelle Animalerie Commune, Pitié-Salpétrière, Paris, France). C57BL/6-TgH (recombinase-activating gene 2 (RAG-2) KO) mice were obtained from Centre de Développement des Techniques Avancées pour l'expérimentation animale (Orléans, France). All these mice are of the normally susceptible H-2^b phenotype. CCR-5 KO mice from The Jackson Laboratory were backcrossed on the C57BL/6 background in our animal facility.

Parasites

Clone 1.49L of the *PbA* strain was a gift from Dr. D. Walliker (Institut of Genetics, Edinburgh, U.K.). This parasite was maintained in C57BL/6 mice and induces ECM, characterized by hemi- or paraplegia, ataxia, deviation of the head, and convulsions between 6–8 days postinfection (14). The erythrocytic stages of the parasite were stocked in liquid nitrogen as

*Institut National de la Santé et de la Recherche Médicale, Unité 511, Immunobiologie Cellulaire et Moléculaire des Infections Parasitaires; †Institut National de la Santé et de la Recherche Médicale, Unité 543, Laboratoire d'Immunologie Cellulaire; and ‡Laboratoire de Neuropathologie Raymond Escourolle, CHU Pitie-Salpétrière, Université Pierre et Marie Curie, Paris, France

Received for publication August 29, 2002. Accepted for publication December 11, 2002.

The costs of publication of this article were defrayed in part by the payment of page charges. This article must therefore be hereby marked *advertisement* in accordance with 18 U.S.C. Section 1734 solely to indicate this fact.

[1] This work was supported by a grant from La Fondation de Treilles (Paris, France; to J.N.) and by Grant PAL+ from Ministère de la Recherche.

[2] D.M. and B.C. contributed equally to this work.

[3] Address correspondence and reprint requests to Dr. Béhazine Combadière and Prof. Dominique Mazier, Institut National de la Santé et de la Recherche Médicale, Unité 543 or Unité 511, CHU Pitie-Salpétrière, Université Pierre et Marie Curie, 91 boulevard de l'Hôpital, 75634 Paris Cedex 13, France. E-mail addresses: mazier@ext.jussieu.fr and combadie@ccr.jussieu.fr

[4] Abbreviations used in this paper: CM, cerebral malaria; ECM, experimental cerebral malaria; KO, knockout; *PbA*, *Plasmodium berghei* ANKA; pRBC: parasitized RBC; RAG, recombinase-activating gene; RT-MPCR, RT-multiplex PCR; WT, wild type.

0022-1767/03/$02.00

parasitized red blood stage (pRBC) per milliliter in Alsever's solution containing 10% glycerol. The parasite infection was induced by i.p. injection of 10^6 pRBCs. Parasitemia was determined daily on Giemsa-stained blood smears and was expressed as the percent parasitemia. We choose to infect the mice with a single dose of 10^6 pRBCs because lower doses (10^2) of parasites were not able to induce ECM in C57BL6 susceptible mice.

Histology

Brains were recovered after perfusion with 1× PBS, formalin fixed, (AFA, fixing liquid; Carlo Erba, Val de Reuil, France) then paraffin-embedded for preparation of histological sections. Five-micrometer-thick sections were cut, stained with H&E, and examined by light microscopy.

Preparation of brain cell suspensions

The brains were obtained from WT susceptible mice at the coma stage of ECM and at the same time from KO animals (day 6). Briefly, brains were removed and homogenized in RPMI 1640 medium (Life Technologies, Cergy Pontoise, France) by passing through sterile meshes to obtain a single-cell suspension. Percoll (Pharmacia Biotech, Uppsala, Sweden) was added at a final concentration of 35%, and cells were centrifuged at 400 × *g* for 20 min at 20°C. The cell pellets were washed twice and subjected to flow cytometric analyses or T lymphocyte enrichment.

Flow cytometric analyses

Brain cells were stained for FACS analysis according to standard protocols in cold 1× PBS containing 2% FCS and 0.01% sodium azide (FACS buffer) with the following Abs: CyChrome-labeled anti-CD4, FITC-labeled anti-CD3 (145-2C11, hamster IgG1), PE-labeled anti-CD4 (H129.19, rat IgG2a), PerCP-labeled anti-CD8α (53-6.7, rat IgG2a), PE-conjugated anti-CD44 (Pgp-1), PE-labeled anti-CD69 (Mel-14), and biotin-labeled CD62L (H1.2F3) mAbs, and streptavidin-allophycocyanin was used at the secondary step (BD PharMingen, France). The whole blood was stained before proceeding to erythrocyte lysis. RBC were eliminated using cell lysis buffer (155 mM NH_4Cl, 10 mM $KHCO_3$, and 0.1 mM EDTA), and cells were washed in FACS buffer. Cells were washed twice before flow cytometric analyses. A total of 10,000–20,000 living events were analyzed using a four-color FACSCalibur flow cytometer with ProCellQuest software (BD Biosciences, Mountain View, CA).

In vivo study of CFSE-labeled cell migration

Splenocytes were prepared from naive and infected mice on day 6 postinfection. Cell suspensions were prepared by passing through sterile meshes. Erythrocytes were lysed using RBC lysis buffer as described above. Cells were washed twice in RPMI 1640 medium (Life Technologies), counted by trypan blue exclusion staining, and adjusted to 10^7 cells/ml. Staining of spleen cells with CFSE (Molecular Probes, Eugene, OR) was performed as described by Lyons and Parish (15). Briefly, cells were resuspended at 1×10^7 cells/ml in 1× PBS. A 5-mM stock solution of CFSE in DMSO was added to a final concentration of 10 μM, and cells were incubated for 30 min at 37°C in a water bath. Cells were washed twice with ice-cold 10% FCS/RPMI 1640 and once with 1× PBS, then resuspended in 1× PBS. Cells were administered i.v. to the mice (5×10^6), and some of these mice were infected 1 h later with 10^6 parasites by the i.p administration route. Single-cell suspensions of brains and spleens of the recipients were analyzed between days 6–8 following adoptive cell transfer.

Adoptive transfer of $CD8^+$ cells

Cell suspensions from the spleen of WT and PFP-KO mice were prepared by the methods described above and pooled, and $CD8^+$ cells were purified with MACS beads according to the manufacturer's instructions (Miltenyi Biotech, Paris, France). Briefly, cells were suspended in MACS buffer and incubated for 15 min at 4°C with magnetic Abs specific for CD8 T cells. Cells were washed, and the suspension was applied to a MACS-MS^+ separation column (Miltenyi Biotech) in an appropriate MACS separator, washed three times, and eluted in 1 ml of MACS buffer. Cells were stained with PerCP-conjugated anti-CD8 Ab, and the purity was evaluated by FACS analysis. After two or three rounds of column separation, we obtained >98% $CD8^+$ T lymphocytes enrichments.

Recipient mice (WT, PFP-KO, or RAG2-KO) were administered i.v. with either total spleen cells or purified $CD8^+$ or $CD8^-$ cells (5×10^6). After 1 h mice were infected i.p. with 10^6 pRBC. Controls included mice that received spleen cells without pRBC.

RT-multiplex PCR (RT-MPCR)

Total RNA was isolated from purified $CD8^+$ T lymphocytes. RT-PCR was performed to evaluate cytokine and chemokine receptor gene expressions. Total RNA was extracted using the QIAamp RNA Blood Mini kit (Qiagen, Courtaboeuf, France). cDNA was generated using the Omniscript Reverse Transcriptase kit (Qiagen). RT-MPCR analysis was performed using the Quantitative PCR CytoXpress Detection kit for mouse cytokines (Mouse Th1/Th2 Set 2 Signaling CytoXpress Multiplex-PCR kit; BioSource, Europe, Montrouge, Belgium), which were designed to detect the expression of IFN-γ, IL-2, IL-4, IL-5, IL-10, IL-12p40, IL-13, and GAPDH genes. The quantitative PCR CytoXpress Detection kit for mouse CXCR and CCR receptors (Mouse CXCR Chemokine Receptors and Mouse CCR Receptor Set 1; BioSource Europe) was designed to detect the expression of mouse CXCR1 and -2, CXCR3, CXCR4, and CXCR5 for the CXCR genes; CCR1, CCR2, CCR3, CCR4, and CCR5 for the CCR genes; and GAPDH genes. cDNA amplification was performed on a automated PerkinElmer DNA thermocycler (model 480; Palo Alto, CA) using the time-temperature profile according to manufacturer's instructions. Following PCR, the amplicons were analyzed in a 2% agarose gel electrophoresis containing ethidium bromide.

Chromium release assays

Standard chromium release assays were performed as previously described (16). Target cells (P815) were labeled with 60 μCi/10^6 cells of $Na_2\,{}^{51}CrO_4$ (Comissariat d'Energie Atomique, Saclay, France) for 2 h at 37°C and washed twice with RPMI 1640 medium. In the CD3-redirected assays, anti-CD3 mAb (UCHT1) was added to target cells (3×10^3) at 5 μg/ml in triplicate to round-bottom 96-well microtiter plates (PolyLabo, Strasbourg, France) before addition of effector cells at various E:T cell ratios. After a 4-h incubation period at 37°C, the supernatants were collected, and chromium release was measured on a gamma counter. Spontaneous ^{51}Cr release values were 15–25% of total incorporated radioactivity. The percentage of specific release ^{51}Cr was calculated as: percentage = 1 − (experimental − spontaneous release/total radioactivity − spontaneous release) × 100.

Statistical analysis

Data handling, analysis, and graphic representation were performed using PRISM 2.01 (GraphPad, San Diego, CA). Statistical analysis was performed by paired two-sample *t* test for means and by the nonparametric Mann-Whitney *U* test. Statistical significance was accepted at $p < 0.05$.

Results

Development of ECM pathogenesis after PbA *infection is dependent on perforin gene expression*

Pioneering studies have shown the requirement for CD8 T cells in the development of ECM pathogenesis (4). However, the mechanisms by which these cells exert their action remain unclear. Fas/Fas ligand and perforin pathways have been clearly implicated in CD8-mediated cytotoxic effector functions against pathogens (17, 18). To determine whether and which cytotoxic functions were required for the development of ECM, C57BL/6 (WT), *lpr*, *gld*, and PFP-KO mice were infected with *PbA* (Fig. 1*a*). Infected WT, *lpr*, and *gld* mice developed ECM between days 6 and 10 postinfection, whereas none of the PFP-KO mice showed any sign of ECM (Fig. 1*a*), but died from anemia with increased parasitemia between days 17 and 28. The development of ECM pathogenesis after *PbA* infection is therefore dependent on perforin gene expression.

To determine histopathologic alterations during ECM pathogenesis, we examined the brains of ECM-susceptible WT mice at the coma stage and those of ECM-resistant PFP-KO resistant mice at the same time (day 6; Fig. 1). Our studies first focused on pRBC that adhere to the endothelium and microvascular destruction, since these events were shown to be a critical step in ECM pathogenesis as described in previous studies (19). In all infected mice, blood vessels were distended, and spaces around them were enlarged in infected WT or PFP-KO mice (Fig. 1*b*, *B* and *D*) compared with normal brains of uninfected-WT mice (Fig. 1*bA*), suggesting severe edema. Most endothelial cells of the microvasculature showed morphologic changes consisting of amoeboid appearance and suggesting activation in infected WT mice as well as in PFP-KO (Fig. 1*b*, *B* and *D*, ▲). The lumens of the unruptured vessels were congested with sequestrated pRBC

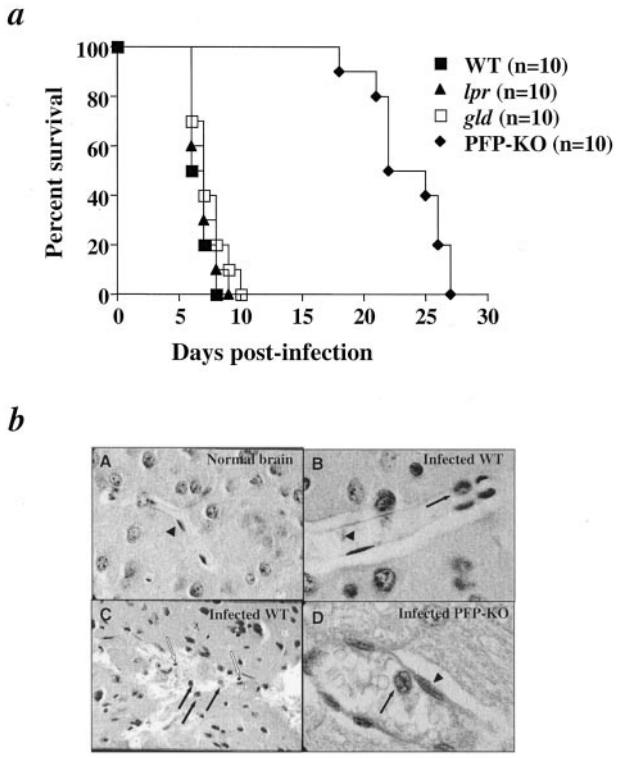

FIGURE 1. The development of ECM pathogenesis after *PbA* infection is dependent on perforin gene expression. *a*, Percent survival of C57BL/6 WT, *lpr*, *gld*, and perforin-deficient (PFP-KO) mice following i.p. *PbA* infection with 10^6 pRBC. The growth rate of parasites was comparable in all strains of mice on day 6 (parasitemia: C57BL6, 5.1 ± 1.5%; *lpr*, 5.6 ± 2.4%; *gld*, 6.2 ± 2.4%; PFP-KO, 4.8 ± 0.8%). Experiments were performed three times with 10 mice in each group. *b*, Histologic analyses of brain sections of ECM-susceptible WT and ECM-resistant PFP-KO mice at the coma stage in WT susceptible mice and at the same time in PFP-KO resistant mice. Brains were removed after perfusion with 1× PBS and were fixed for histological examinations. *A*, Section of a normal mouse brain showing a healthy uninterrupted blood vessel with normal architecture and integrity (magnification, ×250). *B*, Sagittal section of a WT mouse brain at the coma stage showing sequestration and cytoadherence of pRBC (filled arrows). Endothelial cells (▲; magnification, ×750). *C*, Severe lesions in the cortex of infected WT mice showing a disrupted vessel, with destruction of endothelial cells, extravascular pRBC (filled arrows), and mononuclear cell infiltration (empty arrows; magnification, ×500). *D*, Sagittal section of infected PFP-KO mouse brain on day 6 postinfection showing cytoadherence to a vessel wall (filled arrow; magnification, ×1000). ▲, Endothelial cells.

adhering to the vessel walls in ECM-susceptible WT mice as well as in ECM-resistant PFP-KO mice (Fig. 1*b*, *B* and *D*, filled arrows). By contrast, differences concerning cell destruction were found between PFP-KO and WT mice. Indeed, widespread microvasculature lesions with death of endothelial cells (Fig. 1*bC*) were only observed in infected-WT mice at the coma stage, but were never observed in PFP-KO mice. Similarly, parasites scattered throughout extravascular spaces were observed only in the brains of infected WT mice, but not in PFP-KO (Fig. 1*bC*, full arrows). Correlated to the cell wall destruction, mononuclear cell infiltrations were observed in these severe brain lesions of infected WT mice (Fig. 1*bB*, empty arrows). Together, these data indicated that the cytoadherence of pRBC observed in both strains of mice was not sufficient to predict brain damage. In this regard, the ECM pathogenesis would be correlated to both mononuclear cell infiltration and endothelial cell destruction. These observations prompted us to investigate the characterization and functions of infiltrating cells.

CD8 and CD4 T lymphocytes infiltrate the brains of WT-susceptible and PFP-KO resistant mice during PbA *infection*

Consistent with the above observations, trafficking of immunocompetent cells has been described in the establishment of the immune response and various disease progressions (6). To quantify and characterize brain-infiltrating mononuclear cells after *PbA* infection, we performed flow cytometric analyses of brain cell suspensions from WT mice at the coma stage (day 6) and of PFP-KO mice on the same day. Representative flow cytometric analyses indicated that the brains from infected WT and PFP-KO mice contained similar percentages of $CD3^+$ cells (8.6 and 7.6%, respectively; Fig. 2*a*). To better enumerate the CD3 cell population in the brain, the absolute number of $CD3^+$ cells was calculated for each mouse. Uninfected control mice contain <2000 $CD3^+$ cells/brain, whereas 48,030 ± 18,450 $CD3^+$ cells/brain were recovered in infected WT mice. These data clearly indicated that lymphocyte accumulation in the brain is a key event during ECM pathogenesis. However, PFP-KO mice did not develop ECM pathogenesis, although 26,800 ± 14,500 $CD3^+$ cells/brain were recovered in these mice. In addition, in PFP-KO mice the absolute number of $CD3^+$ cells tended to increase at later time points (data not shown). The number of accumulating CD3 cells in the brain was not significantly different in WT and PFP-KO mice ($n = 4$; $p = 0, 11$). These data demonstrated for the first time that $CD3^+$ T lymphocytes infiltrated the brains of both WT-susceptible and PFP-KO resistant mice after *PbA* infection. Furthermore, these results suggest that 1) lymphocyte infiltration is an active phenomenon that does not result from nonspecific leakage of blood cells to the brain after alteration of blood-brain barrier; and 2) although required, the presence of T cell is not sufficient to induce brain damage.

To further investigate potential differences between various subsets of T lymphocytes in infected PFP-KO resistant vs WT susceptible mice, we evaluated absolute numbers of $CD4^+$ and $CD8^+$ cells (Fig. 2). Representative flow cytometric analyses of CD4 and CD8 cells showed 5.3 and 4.5% of $CD8^+$ cells and 2.8 and 3% of $CD4^+$ cells in infected-WT and PFP-KO, respectively. Both WT susceptible and PFP-KO resistant mice had similar percentages and absolute numbers of $CD4^+$ T cells present within the brain cell suspension (3.7 ± 1.9% (14,080 ± 8,570 $CD4^+$ cells/brain) and

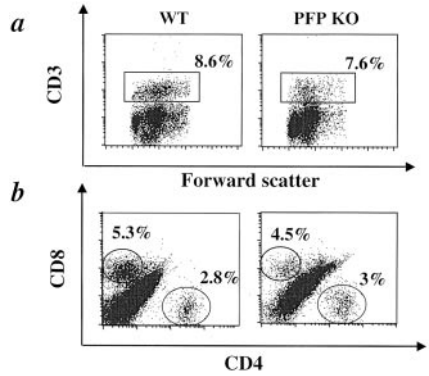

FIGURE 2. CD8 and CD4 T lymphocytes infiltrate the brains of WT susceptible and PFP-KO resistant mice during *PbA* infection. Flow cytometric analyses of CNS-infiltrating lymphocytes in C57BL/6 WT susceptible and PFP-KO resistant mice infected with *PbA*. *a*, CD3 staining in the brain of WT at the coma stage and in PFP-KO mice on day 6 postinfection. *b*, CD4 and CD8 T cells in brains of WT and PFP-KO mice after infection with *PbA*. The percentage positive is indicated.

3.4 ± 1% (11,040 ± 7,350 $CD4^+$ cells/brain), respectively; $n = 4$; $p = 0.9$). The percentages and absolute numbers of CD8 T cells were also similar in WT mice with CM (8.6 ± 4.8% (33,320 ± 23,230 $CD8^+$ cells/brain) and in PFP mice without ECM on day 6 postinfection (7.4 ± 2.3% (20,390 ± 9,172 $CD8^+$ cells/brain); $n = 4$; $p = 0.4$). The absolute numbers of brain-infiltrating $CD8^+$ cells were, on the average, 2-fold higher than those of CD4 cells in both groups of mice. These results were consistent with the total number of $CD3^+$ cells infiltrating the brain. In conclusion, despite differences between WT and PFP-KO mice in their susceptibility to develop ECM, no significant differences were found in the accumulation of CD8 and CD4 T lymphocytes in the brains of these two strains of mice after *PbA* infection.

Brain-infiltrating CD8 and CD4 T lymphocytes in WT-susceptible and PFP-KO-resistant mice are differentiated memory T lymphocytes

We then further evaluated the differentiation and activation status of brain-infiltrating CD8 and CD4 lymphocytes of *PbA*-infected WT mice at the coma stage and PFP-KO mice on day 6 postinfection. As shown in a representative flow cytometric analysis (Fig. 3*a*), brain-infiltrating CD8 were mainly effector/memory T cells, $CD44^+CD62L^-$ (60 and 50%, in WT and PFP-KO mice, respectively). Averages of 56.8 ± 6.6 and 52.7 ± 6% of $CD8^+CD44^+CD62L^-$ cells were detected in WT and PFP-KO mice, respectively (Fig. 3*b*). Similar results were observed for CD4 cells, with averages of 56.8 ± 18.2 and 56.3 ± 5.8% of $CD4^+CD44^+CD62L^-$ cells in WT and PFP-KO mice, respectively (Fig. 3*b*). No naive $CD44^-CD62L^+$ cells were detected in the brains of these mice (Fig. 3*b*). In addition, the majority of CD4 (65–70%) and CD8 (58–70%) cells also expressed the CD69 activation marker (data not shown). No significant differences were observed between these two strains of mice regarding the differentiation and activation status of T lymphocytes. These results together showed that brain-infiltrating CD8 and CD4 cells were mainly differentiated memory cells in both WT susceptible and PFP-KO resistant mice after *PbA* infection.

We then compared these data to the distribution of differentiated memory subsets in the periphery of infected WT and PFP-KO: peripheral blood (Fig. 3*b*), spleen, and lymph nodes (data not shown). Both naive ($CD44^-CD62L^+$) and memory ($CD44^+CD62L^-$) cells were detected in the peripheral blood of infected mice (Fig. 3*a*), whereas no naive cells were found in the brains of infected mice. A major increase in $CD44^+CD62L^-$ cells (Fig. 3*b*) and CD69 (data not shown) was observed in infected mice on day 6 postinfection compared with uninfected mice for both CD8 and CD4 subsets. However, a lower frequency of $CD8^+$ or $CD4^+$ $CD44^+CD62L^-$ PBL was detected in PFP-KO mice than in WT mice after *PbA* ($n = 5$; $p < 0.005$; Fig. 3*b*). Similar results were found in the spleen and lymph nodes of WT susceptible and PFP-KO resistant mice (data not shown). Thus, activated-differentiated CD4 and CD8 T cells similarly infiltrated the brains of both WT-susceptible and PFP-KO mice after *PbA* infection. It can be hypothesized from these findings that T lymphocytes first became activated and differentiate in the periphery and then migrate to the brains of *PbA*-infected mice.

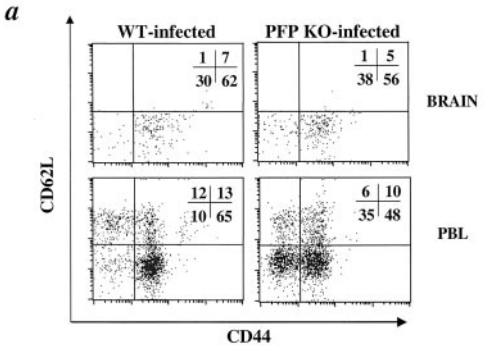

b

BRAIN (n = 3)	CD44+CD62L-	
	CD8+ cells	CD4+ cells
infected WT	56.8±6.6%	56.8±18.2%
infected PFP-KO	52.7±6.0%	56.3±5.8%
	ns	ns

PBL (n=5)	CD44+CD62L-	
	CD8+ cells	CD4+ cells
uninfected WT	14.4±1.2%	14.7±5.6%
Infected WT	64.0±9.0%	44.0±3.5%
	P<0.05	P<0.05
uninfected PFP-KO	16.0±0.5%	16.0±2.3%
Infected PFP-KO	44.0±7.2%	37.7±1.0%

FIGURE 3. Brain-infiltrating CD8 and CD4 T lymphocytes in WT susceptible and PFP-KO resistant mice are differentiated memory T lymphocytes. *a*, Representative flow cytometric analyses of CNS-infiltrating lymphocytes and PBL in WT-susceptible (coma stage) and PFP-KO resistant mice infected with *PbA* on day 6. The analysis of CD44 and CD62L expression was gated on $CD8^+$ cells: *upper panels*, brain; *lower panels*, PBL. *B*, Frequencies of $CD62L^-CD44^{high}$ memory CD4 and CD8 cells were measured in the brain (three pools of three brains) and PBL ($n = 5$) of WT (coma stage) and PFP-KO mice on day 6. The *p* values are indicated.

Following the above hypothesis, we tested whether 1) activated and differentiated cells can migrate to the brain; 2) such migration is dependent on the presence of parasites; 3) a similar phenomenon occurs in WT and PFP-KO mice; and 4) T lymphocyte migration to the brain is involved in the onset of ECM pathology. We then performed a series of adoptive transfer experiments with CFSE-labeled splenocytes from WT mice infected with *PbA* on day 6 postinfection. Recipient mice were either WT susceptible or PFP-KO resistant mice that were infected with parasites 1 h after cell transfer. CFSE-labeled cells were tracked 6 days later in brains and spleens (Fig. 4*a*) of the recipient mice at the coma stage on day 6 postinfection. The results showed an infiltration of $CFSE^+$ lymphocytes in the spleens and brains of both infected WT and PFP-KO mice. Approximately 1–2% of $CFSE^+$ cells were recovered from the spleens, while 0.1–0.2% $CFSE^+$ cells were recovered from the brains, of WT and PFP-KO recipients (Fig. 4*a*). When CFSE-labeled splenocytes from infected WT mice were transferred into uninfected WT recipients, no $CFSE^+$ cells were found in the brains of these mice (Fig. 4*a*), and the mice did not develop ECM. These results indicate that the presence of parasite in the recipient mice was necessary for brain infiltration and disease induction. In addition, naive CFSE-labeled splenocytes (from uninfected WT mice) migrated to the spleen, but not to the brain, of infected WT mice (Fig. 4*a*). Furthermore, 70% of CFSE-labeled cells isolated from infected WT mice were activated CD62L-$CD44^+$. These results were consistent with the absence of the naive cell phenotype in the brain.

A striking consequence of these adoptive transfer experiments was that PFP-KO mice developed ECM pathogenesis and died at the same rate as WT mice (Fig. 4*b*). Thus, ECM was induced in PFP-KO mice after adoptive transfer of cells from infected WT mice, which were directed to the brain of PFP-KO mice. These results further highlight the importance of lymphocyte trafficking to the CNS after *PbA* infection in the development of ECM and suggest that only activated lymphocytes expressing perforin from infected mice can induce ECM pathology. These data prompted us

CFSE-labeled immune splenocytes from WT mice infiltrate the CNS of PFP-KO mice and induce ECM pathology

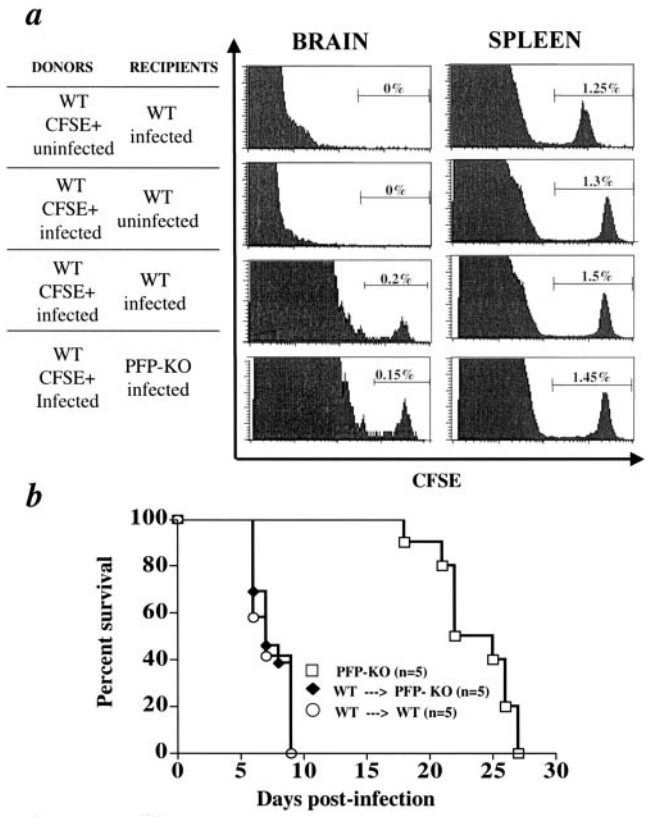

FIGURE 4. CFSE-labeled immune splenocytes from WT mice infiltrate the CNS of PFP-KO mice and induce ECM pathology. *a*, CFSE-labeled Splenocytes (5×10^6 cells/mice) were prepared from *PbA*-infected or uninfected WT mice on day 6 postinfection and adoptively transferred into infected or uninfected WT or PFP-KO recipient mice as indicated. Recipient mice were then infected with 10^6 pRBC. Flow cytometric analyses of $CFSE^+$ cells gated on live lymphocytes infiltrating the brain (*left panel*) and the spleen (*right panel*) of WT and PFP-KO recipient mice on day 6 postinfection. Percentages of cells recovered from the brain and spleen are indicated. *b*, Percent survival of PFP-KO or recipient WT or PFP-KO mice ($n = 5$) after adoptive transfer of CFSE-labeled WT splenocytes (i.v. injection of 5×10^6 cells/mice). Recipient mice WT or PFP-KO mice died from ECM, and PFP-KO mice died after day 21 from anemia. The *p* values are indicated.

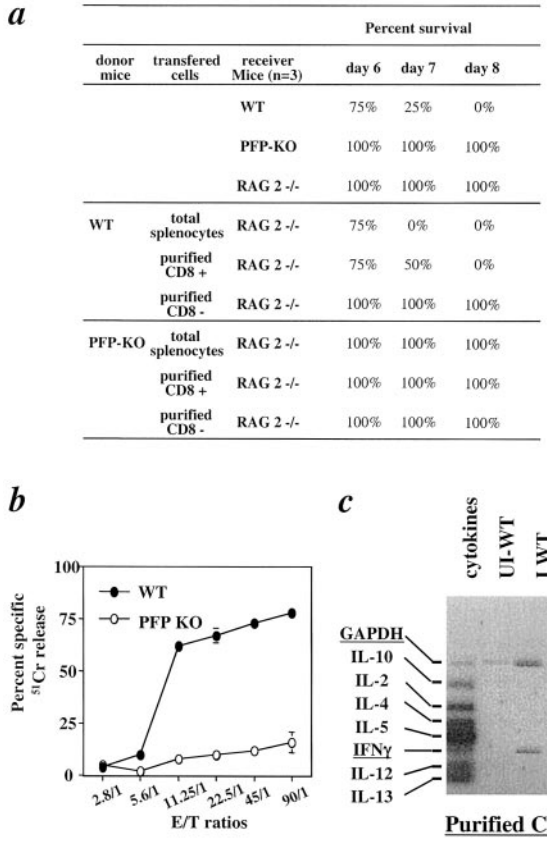

FIGURE 5. Perforin-associated cytolytic mechanisms are required for the development of ECM pathogenesis. *a*, Percent survival of recipient RAG2-KO mice after adoptive transfer of total, $CD8^-$, or $CD8^+$ splenocytes (i.v. injection of 5×10^6 cells/mice) isolated from infected WT or PFP-KO mice on day 6 postinfection. Recipient mice ($n = 3$) were infected 1 h after cell transfer with 10^6 pRBC. Purified $CD8^+$ fractions contained 98–99% $CD8^+$ lymphocytes, as assessed by flow cytometric analyses. *b*, Anti-CD3-redirected chromium release assay of purified $CD8^+$ effector cells from WT and PFP-KO infected mice (E, effector cells). Target cells (T) were from the P815 cell line. *c*, IFN-γ, IL-2, IL-4, IL-5, IL-10, IL12-p40, IL-13 cytokine, and GAPDH gene expression determined by RT-MPCR with $CD8^+$ T cells from WT and PFP-KO infected mice.

to further characterize the cytotoxic/effector capacities of CD8 lymphocytes from infected WT and PFP-KO mice.

Cytotoxic CD8 lymphocytes are required for the development of ECM pathogenesis

The initial observation of the resistance of PFP-KO mice to ECM together with the major infiltration of CD8 and CD4 cells in the brain suggest that mostly cytotoxic mechanisms were involved in the development of ECM. We further tested the capacity of $CD8^+$ and $CD8^-$ subsets to induce ECM and characterize their cytolytic functions and cytokine mRNA expression. We chose RAG2-KO mice because these mice lack peripheral T and B lymphocytes and did not develop ECM (Fig. 5*a*). After infection with *PbA*, RAG2-KO mice died from anemia with increased parasitemia between days 20 and 28 postinfection (data not shown). Splenic $CD8^+$ (purity, ~99% CD8 cells, as assessed by flow cytometric analysis) and CD8 cells from WT mice on day 6 postinfection were magnetically sorted and adoptively transferred into ECM-resistant, RAG2-KO recipient mice (Fig. 5*a*). RAG2-KO recipient mice were then infected with parasites. RAG2-KO became moribund, with all signs of ECM pathogenesis, after adoptive transfer of either total splenocytes or $CD8^+$ cells, but not after transfer of $CD8^-$ cells from infected WT donors (Fig. 5*a*). In addition, RAG2-KO mice did not develop the ECM pathology after adoptive transfer of $CD8^+$ cells isolated from PFP-KO donor mice (Fig. 5*a*). These results demonstrated that only perforin gene-expressing CD8 cells were able to induce ECM.

To further explore functional differences between CD8 cells from PFP-KO and WT mice, we tested their effector functions, such as cytolytic capacity (Fig. 5*b*) and IFN-γ expression (Fig. 5*c*). Because the Ag specificity of the CD8 T cells in *PbA* infection was unknown, we used a CD3-redirected assay to analyze their cytotoxic capacity in a chromium release assay. We showed that in vivo stimulated CD8 T cells from *PbA*-infected WT mice exhibited significantly higher cytotoxicity toward P815 targets than CD8 T cells from PFP-KO mice (80 vs 16% cytotoxicity, respectively; Fig. 5*a*). Naive CD8 T cells from uninfected mice did not mediate any cytotoxic functions (<5% at 90/1 E:T cell ratio). The low level of cytotoxic activities observed with CD8 T cells from PFP-KO mice could be due to Fas/Fas-ligand-induced cytotoxic pathways (17). The cytokine expression was also analyzed by RT-MPCR (Fig. 5*c*). We showed that IFN-γ mRNA was expressed in CD8 cells from both infected WT and PFP-KO, but not in naive CD8

from uninfected mice (Fig. 5). These results demonstrated that in vivo stimulated CD8 T cells from WT mice did not differ from those of PFP-KO mice in their cytokine expression, but differed in their cytolytic capacity.

Brain-infiltrating effector-memory cytotoxic CD8 T cells express chemokine receptor gene, which could be partially involved in the development of ECM pathogenesis

Our above data indicated that activated and differentiated cytotoxic CD8 cells migrated and accumulated in the brain during ECM pathogenesis. The role of chemokines/chemokine receptors in cell trafficking has been described during the establishment of the immune response and disease progression (6). To better understand how CD8 T cells were targeted to the CNS following *PbA* infection, we studied the pattern of chemokine receptor expression on purified $CD8^+$ T cells recovered from spleens (Fig. 6*a*) and brains (Fig. 6*b*) of mice at the coma stage of ECM and at the same time from PFP-KO mice (data not shown). We found that activated $CD8^+$ cells showed increased expression of mRNA coding for CCR-2 and CCR-5 as well as CXCR-3 and CXCR-4, whereas naive CD8 cells (uninfected WT mice) expressed only CXCR4. A similar pattern of chemokine receptor expression was observed in $CD8^+$ cell fractions from both infected WT or PFP-KO mice regardless of their origins, spleen or brain (Fig. 6, *a* and *b*). We thus investigated the role of the chemokine receptor, CCR-5, in ECM pathogenesis using CCR5-deficient ($CCR5^{-/-}$) mice and their littermates ($CCR5^{+/+}$; Fig. 6*c*). We found a modest, but consistent, delayed effect of CCR5-KO on the onset of ECM after *PbA* infection ($n = 10$; $p = 0.0007$). Although limited to the study of one chemokine receptor, these data indicate for the first time the role of these molecules in ECM pathogenesis and emphasize the importance of CD8 cells with regard not only to their cytotoxic capacities, but also to their specific pattern of migration after *PbA* infection.

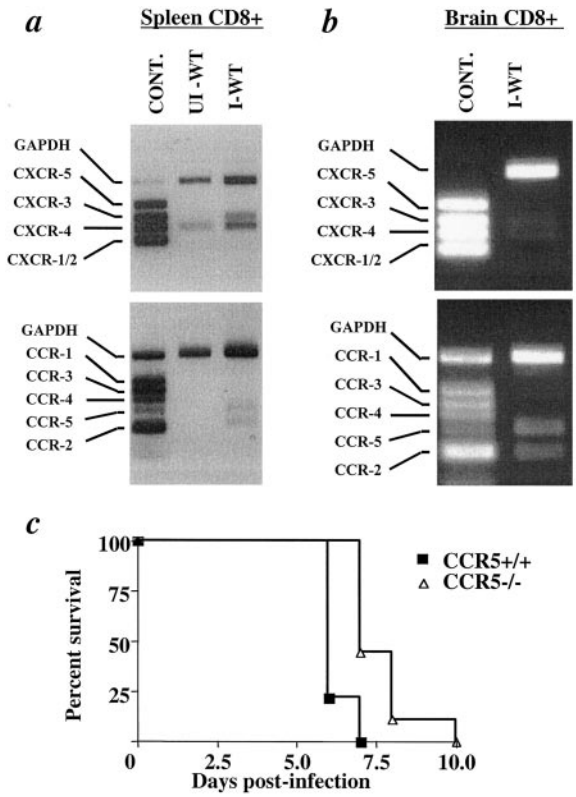

FIGURE 6. Brain-infiltrating effector-memory cytotoxic CD8 T cells express the chemokine receptor gene, which could be partially involved in the development of ECM pathogenesis. Pattern of chemokine receptor expression in brain (*a*) and spleen (*b*) $CD8^+$ T lymphocytes (98% purity) from *PbA*-infected WT mice at the coma stage. Similar results were observed with $CD8^+$ cells from PFP-KO mice (data not shown). RT-MPCR for CXC (*upper panel*) and CC (*lower panel*) chemokine receptors: CXCR1, -2, -3, -4, and -5; CCR1, -2, -3, -4, and –5; and GAPDH. *c*, Percent survival of CCR5-deficient mice and CCR5 WT littermates after infection with *PbA* ($n = 10$; $p = 0.0007$). Mice died from ECM pathogenesis.

Discussion

Our data brought striking evidence of the implication of brain-infiltrating cytotoxic effector CD8 lymphocytes in the development of ECM pathogenesis. We found that in contrast to ECM-susceptible C57BL6 mice, PFP-KO mice were resistant to ECM in absence of brain lesions, whereas cytoadherence of parasitized erythrocytes and a massive accumulation of activated/effector CD8 lymphocytes were observed in both groups of mice. ECM can be induced in PFP-KO mice when cytotoxic CD8 cells from infected C57BL6 mice infiltrated the brain of PFP-KO mice. This specific recruitment might involve chemokine/chemokine receptors, since their expression was up-regulated on activated CD8 cells, and susceptibility to ECM was delayed in CCR5-KO mice.

PFP-KO mice were totally resistant to ECM pathogenesis, whereas mice with mutations in Fas or Fas ligand genes remained susceptible. Indeed, granule exocytosis and Fas/Fas ligand activation pathways are two distinct mechanisms involved in the death of infected target cells by CD8 lymphocytes (17, 20). The Fas-mediated pathway, mainly operative with CD4 T cells, is thought to be primarily involved in immune regulation and maintenance of tolerance (21). Granule exocytosis is mediated by perforin and granzymes and plays a major role in the control of infection (22). Our results clearly demonstrated that perforin-dependent, but not Fas/Fas ligand-dependent, cytotoxic pathways were involved in ECM pathogenesis. Previous reports have observed the resistance of PFP-KO mice to ECM. However, the mechanism involved was not investigated (23). Perforin-mediated cytolysis is the primary pathway of cytotoxicity used by both CD8 T cells and NK cells (22); however, the role of NK cells in the development of ECM has been excluded by Yanez et al. (4). These results together with previous data on the requirement for CD8 cells in the development of ECM (4, 5) further suggest that mainly $CD8^+$ T cells are critical in T cell-mediated immune responses after *PbA* infection and its neurological consequence.

This report is the first demonstration of a massive accumulation of CD8 and CD4 T lymphocytes in the brains of both C57BL/6 and PFP-KO mice on day 6 postinfection. Although most of our studies showed results on day 6, we have also investigated cell infiltration on days 10 and 15 postinfection in perforin KO mice. We found 2-fold increased cell infiltration of both $CD4^+$ and $CD8^+$ T cells in the brains of PFP KO mice on days 10 and 15 postinfection compared with day 6 (data not shown). These mice did not develop cerebral symptoms, but did later with overwhelming parasitemia. Hence, the number of infiltrating T cells was indicative not of disease induction, but, rather, of perforin expression by $CD8^+$ T cells. Our results provide striking evidence that T lymphocytes were mainly activated and differentiated specifically recruited to the brain as ascribed by CD44, CD69 up-regulation, and CD62L down-regulation. We found that T cell memory also increased in the periphery (PBL, spleen, and lymph nodes) of *PbA*-infected WT and PFP mice. However, the memory cell population was less expanded in PFP-KO than in WT mice. It has been demonstrated

that the acquisition of perforin-dependent cytotoxic activity regulates the expansion and persistence of CD8 effector T cells in vivo (24, 25). This mechanism is independent of the role of perforin as an antimicrobial effector molecule (25). Thus, the survival and death of CD8 cells might be differently regulated in the peripheral blood of WT and PFP-KO mice after *PbA* infection.

Our work clearly indicated that lymphocyte accumulation in the brain is a key event during ECM pathogenesis. Infected WT mice developed ECM with severe brain damage, whereas PFP-KO mice did not develop ECM pathogenesis, while T lymphocytes also accumulated in brains. Thus, the lymphocyte infiltration is an active phenomenon that did not result from alteration of the blood-brain barrier. Adoptive transfer of CFSE-labeled splenocytes from infected WT or PFP-KO recipient mice revealed preferential migration of $CFSE^+$ lymphocytes into the brain after the host parasite infection. In addition, ECM pathogenesis can be induced in PFP-KO mice when cytotoxic $CD8^+$ cells from infected C57BL6 mice infiltrated the brain of PFP-KO mice. Although CD8 T lymphocytes produced IFN-γ, its secretion by these cells was not sufficient for the development of ECM. As a matter of fact, when PFP-KO $CD8^+$ cells, which also produce IFN-γ, were transferred in vivo, mice remained resistant to ECM. It has also been shown that IFN-γ receptor KO mice (26) and IFN-γ KO mice (J. Nitcheu, unpublished observation) were resistant to the development of ECM pathogenesis. IFN-γ produced by other types of cells could play a role in ECM. Indeed, IFN-γ was shown to be required for *PbA*-induced endothelial ICAM-1 up-regulation (27), which might be involved in the interaction of effector CD8 lymphocytes with APC.

We have shown that several conditions are required for the onset of ECM: 1) infiltration of CD8 lymphocytes in the brain, 2) cytotoxic capacity of infiltrating CD8 lymphocytes, and 3) presence of parasites in mice. The recent definition of murine endothelial cells as semiprofessional APC (28) led us to speculate that these cells are likely to play a role in Ag presentation. Previous reports have implicated the role of ICAM-1 in the induction of ECM, suggesting that the interaction of effector to APC was a crucial step in the pathogenesis (29). The striking histological differences between the two strains of mice concerned the severe destructive lesions selectively affecting WT brain microvessels, with disrupted microvessels and widespread endothelial cell destruction. Therefore, Ag presentation by endothelial cells to inflammatory T CD8 cells was likely to occur and might lead to endothelial cell destruction. Furthermore, histopathologic examinations in WT susceptible and PFP-KO resistant mice showed similar tendencies: cytoadherence of sequestrated pRBC to the endothelium of cerebral vessels and activation of endothelial cells. In many studies sequestration of cells within the microvasculature has been invoked as a factor of pathology leading to vessel occlusion (14). In our study we showed that the cytoadherence phenomenon occurred in both resistant and susceptible mice and thus was necessary, but not sufficient, to induce ECM pathology.

The multistep process of leukocyte binding to endothelium occurred through complex interactions of adhesion molecules, chemoattractants, and their receptors, including cell rolling, adherence, diapedesis, and migration (30–32). The pattern of chemokine receptor expression on cytolytic effector cells compared with naive CD8 cells showed for the first time increased expression of CCR2, CCR5, and CXCR3 that could be involved in the preferential migration of peripheral T lymphocytes to the brain. A similar pattern of receptor expression was observed in both infected PFP and WT mice. Several ligands of these receptors might be expressed in the brain during inflammation (10, 13, 33–37). Although CXCR4 is relevant in the trafficking of all resting and activated lymphocytes, CXCR3, CCR2, and CCR5 expressions were likely to be involved in the recruitment of activated T cells in multiple tissues, including the brain, during neuropathologic disorders (33). CCR5, CXCR3, and their ligands, macrophage inflammatory protein-1α and IFN-γ-inducible protein 10, have been recently implicated in activated T cell migration to the CNS in demyelinating brain lesions (36). Since CCR-5 is expressed on type 1 CTLs, we chose to study available CCR5-KO mice as a first example of the functional role for these chemokine receptors. A consistent effect was found on ECM onset after *PbA* infection in CCR5-KO mice. Other chemokine receptors might play a synergistic role, since the onset of ECM was delayed, but not abolished, in CCR5-KO mice. Although these data should be expanded to the study of CXCR3 and CCR2 in this pathology, we think our results open new perspectives in the involvement of cell trafficking of cytotoxic/effector cells in the brain during ECM pathogenesis after *PbA* infection.

Acknowledgments

We thank O. Sylvie and S. Bagot for technical assistance. We also thank P. Delis for supervising the animal care facility Nouvelle Animalerie Commune de la Pitié-Salpétrière. We are particularly grateful to Profs. P. Debre, B. Autran, and J. C. Ameisen for helpful discussions.

References

1. World Health Organization, Division of Control of Tropical Diseases. 1990. Severe and complicated malaria. *Trans. R. Soc. Trop. Med. Hyg. 84:1.*
2. Lou, J., R. Lucas, and G. E. Grau. 2001. Pathogenesis of cerebral malaria: recent experimental data and possible applications for humans. *Clin. Microbiol. Rev. 14:810.*
3. Finley, R. W., L. J. Mackey, and P. H. Lambert. 1982. Virulent *P. berghei* malaria: prolonged survival and decreased cerebral pathology in cell-dependent nude mice. *J. Immunol. 129:2213.*
4. Yanez, D. M., D. D. Manning, A. J. Cooley, W. P. Weidanz, and H. C. van der Heyde. 1996. Participation of lymphocyte subpopulations in the pathogenesis of experimental murine cerebral malaria. *J. Immunol. 157:1620.*
5. Boubou, M. I., A. Collette, D. Voegtle, D. Mazier, P. A. Cazenave, and S. Pied. 1999. T cell response in malaria pathogenesis: selective increase in T cells carrying the TCR V(β)8 during experimental cerebral malaria. *Int. Immunol. 11: 1553.*
6. Gerard, C., and B. J. Rollins. 2001. Chemokines and disease. *Nat. Immunol. 2:108.*
7. Elhofy, A., K. J. Kennedy, B. T. Fife, and W. J. Karpus. 2002. Regulation of experimental autoimmune encephalomyelitis by chemokines and chemokine receptors. *Immunol. Res. 25:167.*
8. Tran, E. H., W. A. Kuziel, and T. Owens. 2000. Induction of experimental autoimmune encephalomyelitis in C57BL/6 mice deficient in either the chemokine macrophage inflammatory protein-1α or its CCR5 receptor. *Eur. J. Immunol. 30:1410.*
9. Tran, E. H., E. N. Prince, and T. Owens. 2000. IFN-γ shapes immune invasion of the central nervous system via regulation of chemokines. *J. Immunol. 164: 2759.*
10. Soriano, S. G., L. S. Amaravadi, Y. F. Wang, H. Zhou, G. X. Yu, J. R. Tonra, V. Fairchild-Huntress, Q. Fang, J. H. Dunmore, D. Huszar, et al. 2002. Mice deficient in fractalkine are less susceptible to cerebral ischemia-reperfusion injury. *J. Neuroimmunol. 125:59.*
11. Kennedy, K. J., and W. J. Karpus. 1999. Role of chemokines in the regulation of Th1/Th2 and autoimmune encephalomyelitis. *J. Clin. Immunol. 19:273.*
12. Kennedy, K. J., R. M. Strieter, S. L. Kunkel, N. W. Lukacs, and W. J. Karpus. 1998. Acute and relapsing experimental autoimmune encephalomyelitis are regulated by differential expression of the CC chemokines macrophage inflammatory protein-1α and monocyte chemotactic protein-1. *J. Neuroimmunol. 92:98.*
13. Glabinski, A. R., M. Tani, V. K. Tuohy, R. J. Tuthill, and R. M. Ransohoff. 1995. Central nervous system chemokine mRNA accumulation follows initial leukocyte entry at the onset of acute murine experimental autoimmune encephalomyelitis. *Brain Behav. Immun. 9:315.*
14. Aikawa, M., M. Iseki, J. W. Barnwell, D. Taylor, M. M. Oo, and R. J. Howard. 1990. The pathology of human cerebral malaria. *Am. J. Trop. Med. Hyg. 43:30.*
15. Lyons, A. B. 2000. Analysing cell division in vivo and in vitro using flow cytometric measurement of CFSE dye dilution. *J. Immunol. Methods 243:147.*
16. Joly, P., J. M. Guillon, C. Mayaud, F. Plata, I. Theodorou, M. Denis, P. Debre, and B. Autran. 1989. Cell-mediated suppression of HIV-specific cytotoxic T lymphocytes. *J. Immunol. 143:2193.*
17. Kagi, D., F. Vignaux, B. Ledermann, K. Burki, V. Depraetere, S. Nagata, H. Hengartner, and P. Golstein. 1994. Fas and perforin pathways as major mechanisms of T cell-mediated cytotoxicity. *Science 265:528.*
18. Kagi, D., P. Seiler, J. Pavlovic, B. Ledermann, K. Burki, R. M. Zinkernagel, and H. Hengartner. 1995. The roles of perforin- and Fas-dependent cytotoxicity in protection against cytopathic and noncytopathic viruses. *Eur. J. Immunol. 25: 3256.*

19. Berendt, A. R., D. J. Ferguson, J. Gardner, G. Turner, A. Rowe, C. McCormick, D. Roberts, A. Craig, R. Pinches, B. C. Elford, et al. 1994. Molecular mechanisms of sequestration in malaria. *Parasitology 108:S19.*
20. Lowin, B., M. Hahne, C. Mattmann, and J. Tschopp. 1994. Cytolytic T-cell cytotoxicity is mediated through perforin and Fas lytic pathways. *Nature 370: 650.*
21. Nagata, S., and P. Golstein. 1995. The Fas death factor. *Science 267:1449.*
22. Kagi, D., B. Ledermann, K. Burki, R. M. Zinkernagel, and H. Hengartner. 1996. Molecular mechanisms of lymphocyte-mediated cytotoxicity and their role in immunological protection and pathogenesis in vivo. *Annu. Rev. Immunol. 14:207.*
23. Potter, S., G. Chaudhri, A. Hansen, and N. H. Hunt. 1999. Fas and perforin contribute to the pathogenesis of murine cerebral malaria. *Redox. Rep. 4:333.*
24. Kagi, D., B. Odermatt, and T. W. Mak. 1999. Homeostatic regulation of $CD8^+$ T cells by perforin. *Eur. J. Immunol. 29:3262.*
25. Badovinac, V. P., A. R. Tvinnereim, and J. T. Harty. 2000. Regulation of antigen-specific $CD8^+$ T cell homeostasis by perforin and interferon-γ. *Science 290: 1354.*
26. Amani, V., A. M. Vigario, E. Belnoue, M. Marussig, L. Fonseca, D. Mazier, and L. Renia. 2000. Involvement of IFN-γ receptor-medicated signaling in pathology and anti-malarial immunity induced by Plasmodium berghei infection. *Eur. J. Immunol. 30:1646.*
27. Rudin, W., N. Favre, G. Bordmann, and B. Ryffel. 1997. Interferon-γ is essential for the development of cerebral malaria. *Eur. J. Immunol. 27:810.*
28. Marelli-Berg, F. M., D. Scott, I. Bartok, E. Peek, J. Dyson, and R. I. Lechler. 2001. Antigen presentation by murine endothelial cells. *Transplant. Proc. 33: 315.*
29. Favre, N., C. Da Laperousaz, B. Ryffel, N. A. Weiss, B. A. Imhof, W. Rudin, R. Lucas, and P. F. Piguet. 1999. Role of ICAM-1 (CD54) in the development of murine cerebral malaria. *Microbes Infect. 1:961.*
30. Springer, T. A. 1994. Traffic signals for lymphocyte recirculation and leukocyte emigration: the multistep paradigm. *Cell 76:301.*
31. Johnston, B., and E. C. Butcher. 2002. Chemokines in rapid leukocyte adhesion triggering and migration. *Semin. Immunol. 14:83.*
32. Kunkel, E. J., and E. C. Butcher. 2002. Chemokines and the tissue-specific migration of lymphocytes. *Immunity 16:1.*
33. Sorensen, T. L., M. Tani, J. Jensen, V. Pierce, C. Lucchinetti, V. A. Folcik, S. Qin, J. Rottman, F. Sellebjerg, R. M. Strieter, et al. 1999. Expression of specific chemokines and chemokine receptors in the central nervous system of multiple sclerosis patients. *J. Clin. Invest. 103:807.*
34. Boztug, K., M. J. Carson, N. Pham-Mitchell, V. C. Asensio, J. DeMartino, and I. L. Campbell. 2002. Leukocyte infiltration, but not neurodegeneration, in the CNS of transgenic mice with astrocyte production of the CXC chemokine ligand 10. *J. Immunol. 169:1505.*
35. Ghersa, P., M. Gelati, J. Colinge, G. Feger, C. Power, R. Papoian, and A. Salmaggi. 2002. MIG: differential gene expression in mouse brain endothelial cells. *NeuroReport 13:9.*
36. Balashov, K. E., J. B. Rottman, H. L. Weiner, and W. W. Hancock. 1999. $CCR5^+$ and $CXCR3^+$ T cells are increased in multiple sclerosis and their ligands MIP-1α and IP-10 are expressed in demyelinating brain lesions. *Proc. Natl. Acad. Sci. USA 96:6873.*
37. Westmoreland, S. V., J. B. Rottman, K. C. Williams, A. A. Lackner, and V. G. Sasseville. 1998. Chemokine receptor expression on resident and inflammatory cells in the brain of macaques with simian immunodeficiency virus encephalitis. *Am. J. Pathol. 152:659.*